

Correlation of ion acoustic turbulence with self-organization in a low-temperature plasma

Cite as: Phys. Plasmas **26**, 082308 (2019); <https://doi.org/10.1063/1.5111552>

Submitted: 27 May 2019 . Accepted: 26 July 2019 . Published Online: 20 August 2019

Marcel P. Georgin , Benjamin A. Jorns , and Alec D. Gallimore



View Online



Export Citation



CrossMark

ARTICLES YOU MAY BE INTERESTED IN

[On the generalized formulation of Debye shielding in plasmas](#)

Physics of Plasmas **26**, 050701 (2019); <https://doi.org/10.1063/1.5091949>

[Announcement: The 2018 Ronald C. Davidson Award for Plasma Physics](#)

Physics of Plasmas **26**, 050201 (2019); <https://doi.org/10.1063/1.5109579>

[Performance of Wendelstein 7-X stellarator plasmas during the first divertor operation phase](#)

Physics of Plasmas **26**, 082504 (2019); <https://doi.org/10.1063/1.5098761>

 **AVS Quantum Science**

AIP Publishing 

A high impact interdisciplinary journal for **ALL** quantum science

ACCEPTING SUBMISSIONS



Correlation of ion acoustic turbulence with self-organization in a low-temperature plasma

Cite as: Phys. Plasmas **26**, 082308 (2019); doi: [10.1063/1.5111552](https://doi.org/10.1063/1.5111552)

Submitted: 27 May 2019 · Accepted: 26 July 2019 ·

Published Online: 20 August 2019



View Online



Export Citation



CrossMark

Marcel P. Georgin,¹ Benjamin A. Jorns,² and Alec D. Gallimore²

AFFILIATIONS

¹Applied Physics Program, University of Michigan, Ann Arbor, Michigan 48109, USA

²Department of Aerospace Engineering, University of Michigan, Ann Arbor, Michigan 48109, USA

ABSTRACT

The correlation between ion acoustic turbulence (IAT) and self-organization is investigated in a low-temperature, current-carrying xenon plasma. Translating probes are used to measure the dispersion and power spectra of relative fluctuations in the ion saturation current in the plume of a hollow cathode discharge. Both ion acoustic waves and a low-frequency, propagating coherent oscillation are detected. Time-resolved measurements reveal that the amplitude of the IAT modes is modulated in time and is highly correlated in space and time with the coherent fluctuations in the ion saturation current and light emission. The phase relationship between the IAT amplitude and these oscillations further suggests that fluctuations in turbulence are causally connected to the periodic, self-organized structure. These results are interpreted in the context of a zero-dimensional model for the electron energy that balances Ohmic heating from the IAT against inelastic losses from ionization. A comparison of the model with the experimental measurements supports the conclusion that this form of self-organization is hydrodynamic in nature but is possibly driven unstable by the presence of kinetic electrostatic turbulence.

Published under license by AIP Publishing. <https://doi.org/10.1063/1.5111552>

I. INTRODUCTION

The appearance of self-organized, low-frequency, propagating plasma structures is a nearly universal phenomenon in plasma physics, occurring in high-density,^{1–5} astrophysical,^{6,7} and low-temperature systems.^{8–10} This process is believed to dictate the plasma state in many of these configurations. Indeed, for low-temperature plasmas (LTPs) in particular, self-organization has been recognized as a critical research frontier in developing a better understanding of this class of plasmas.¹¹ While several experiments and numerical studies have investigated this process in LTPs,^{8–10,12} the mechanisms underlying self-organization in many cases remain unclear. An intriguing theory that has recently gained renewed interest is the possibility that these self-organized structures are the product of a unique, inverse energy transfer across lengthscales.^{13,14} In particular, the growth of a small-wavelength, kinetically driven electrostatic turbulence could couple to and ultimately result in the coalescing of self-organized states in LTPs.^{15,16} Despite the ongoing theoretical work that points to this possibility, there have been only a few experimental studies that have attempted to link turbulence in LTPs and self-organization.^{8–10} Given the demand for a better understanding of the plasma state in LTPs, the broad interest of self-organization, and the possibility that this phenomenon occurs through a unique mechanism, there is a pressing need for further experimental investigation of this process. This article

presents a detailed study of the role of plasma turbulence in promoting self-organization in a current-carrying, unmagnetized.

To examine this fundamental connection, we use a thermionic hollow cathode test-article. This device generates a current-carrying plasma state that is well known to be dominated by the effects of ion acoustic turbulence (IAT)^{17–22} and has been used in a number of fundamental studies.^{23–29} It has been established²⁷ that a form of self-organization can also be excited by reducing the gas flow rate at a constant current. The resulting structure is characterized by coherent, large-scale fluctuations in potential and density that can propagate in space with typical frequencies between 10 and 100 kHz. Initial investigations of this so-called “plume-mode” indicate this macroscopic behavior is limited to the external plasma plume, away from the cathode sheath,²⁷ and that this state coexists with the IAT. However, there is no experimental evidence directly tying these two instabilities. Building on the extensive list of fundamental work into basic processes in LTPs emerging from the study of hollow cathodes, this article examines, for the first time, the correlational and potentially causal link between self-organization and underlying turbulence in current-carrying LTPs.

This paper is organized in the following way: Sec. II contains a description of the experimental apparatus and plasma diagnostics. In Sec. III, we present the results of the experiment along with a description of the analysis techniques to correlate the self-organized mode with fluctuations in electrostatic turbulence. To interpret our results,

we develop a zero-dimensional model in Sec. IV and compare it with the experiment in Sec. V.

II. EXPERIMENTAL SETUP

Figure 1 shows the experimental test configuration. This 20-A BaO hollow cathode uses a tungsten orifice and a graphite keeper electrode³⁰ and was installed in a 1 m × 1 m vacuum chamber with an operating pressure of 20 μTorr. The plasma discharge was established between the cathode and a cylindrical anode located a distance $\ell = 38$ mm downstream of the cathode's exit. We operated the source at 22.5 A and 19.0 V with a 10 sccm flow rate of xenon (see Fig. 3).

To measure both coherent and incoherent waves, we used two diagnostics, a high-speed camera and cylindrical Langmuir probes. The camera captured the characteristic fluctuations in the light intensity of the plasma plume through an optical viewport. The images were acquired at 480 kfps. We measured ion saturation current oscillations in the plume of the test-article with a pair of ion saturation probes, a common technique for characterizing oscillations in LTPs.^{28,29,31–33} These cylindrical probes, 3 mm long and 0.5 mm in diameter, were spaced 5.2 mm apart, oriented perpendicularly to the flow, and biased to -36 V below ground. The large-scale oscillations also drove variations in the total discharge current to the cathode, which we simultaneously measured. As outlined in the following, this latter signal served as a trigger reference for time-resolved analysis. Both the ion saturation and discharge current signals were acquired at 10 MS/s for 100 ms at each position.

III. RESULTS AND ANALYSIS

A. Time-averaged measurements

We show direct measurements of the time-averaged density and electron temperature with a swept and translating Langmuir probe in Fig. 2. The density decreased monotonically from $\mathcal{O}(10^{18})$ to $\mathcal{O}(10^{17})$ m⁻³ with distance from the cathode while the temperature increased monotonically from 1.5 to 2.2 ± 0.2 eV. Thus, the Debye length was on the order of 1–10 μm and the ion plasma frequency was between 100 and 200 MHz. This is consistent with other measurements of time-averaged plasma parameters in hollow cathodes.^{27,34}

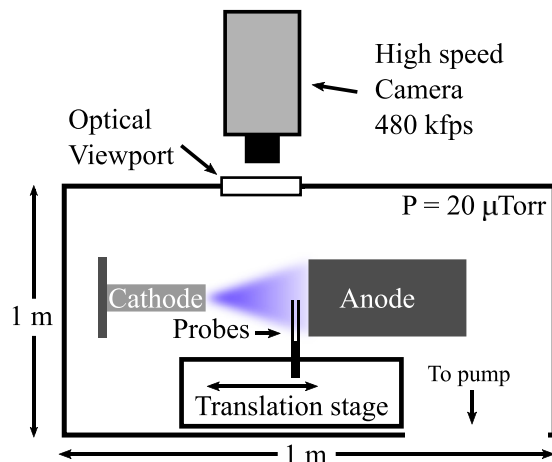


FIG. 1. Experimental configuration showing the vacuum facility, cathode, anode, probes, and high-speed camera. The operating background pressure is 20 μTorr.

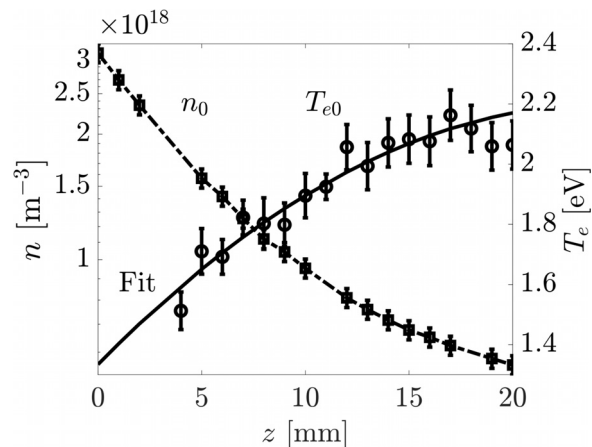


FIG. 2. Steady state density and electron temperature calculated from Langmuir probe traces.

The time-dependent properties we subsequently report fluctuate against this steady-state background.

B. High-speed imaging

As a first metric for characterizing these time-dependent properties, we show in Fig. 3 the results for variations in the light intensity

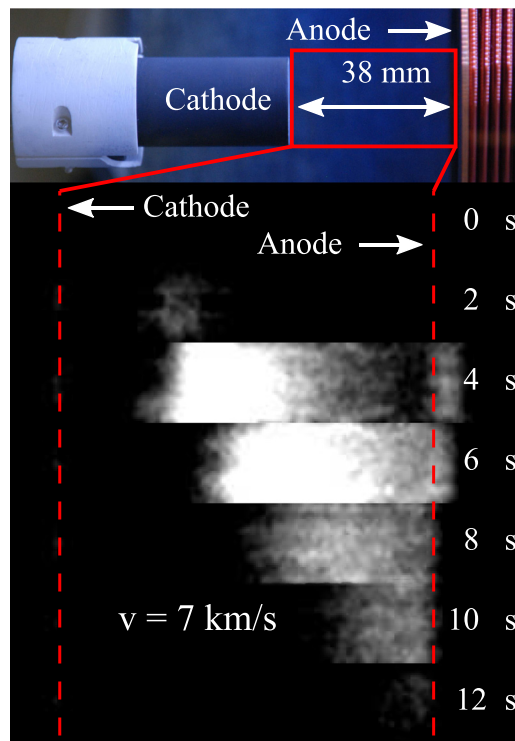


FIG. 3. BaO hollow cathode in the vacuum facility. High-speed camera frames are captured at 480 kfps. One cycle of oscillation is 13 frames or ~36 kHz.

measured with the high-speed camera. These image stills qualitatively show the periodic formation of the self-organized structure. This is, to our knowledge, one of the first series of time-resolved images of the so-called plume mode and reveals, qualitatively, insights into its structure. In particular, we can see that the oscillation appears to originate at a fixed spatial location near the cathode where light is periodically emitted at 36 kHz (a frequency also observed in the discharge current). It then propagates at 7 km/s toward the anode. Ultimately, this change in the light intensity is indicative of the relatively coherent density and/or temperature fluctuations in the plasma.

C. Probe-based power spectra

To quantify this oscillatory behavior, we show in Fig. 4, at three positions, the power spectrum of relative ion saturation current fluctuations, $(\tilde{I}/I_0)_\omega^2$, where I_0 is the time-averaged ion saturation current, \tilde{I} is the fluctuation, and ω is the frequency. This figure indicates the presence of the two classes of instabilities that have been previously identified in the plasma generated by these cathodes: self-organized, low-frequency, coherent oscillations and high-frequency, broadband waves that were linked with IAT.^{17,28,29,35} Near the cathode, the plasma is dominated by the low-frequency oscillation. The spectrum is characterized by a series of monotonically decreasing harmonics with a fundamental frequency of $f_0 = 36$ kHz, which is consistent with oscillations in the discharge current and with the light emission in Fig. 3. This spectral structure is indicative of nonsinusoidal, periodic behavior. Downstream, the amplitude of the high-frequency oscillations (between 100 and 1500 kHz) rises. The dissipation at higher frequencies of these waves follows a power law dependence on frequency, with the exponents between -1.5 and -2.7 . These two trends are consistent with earlier work in Refs. 28 and 29 on IAT in cathodes.

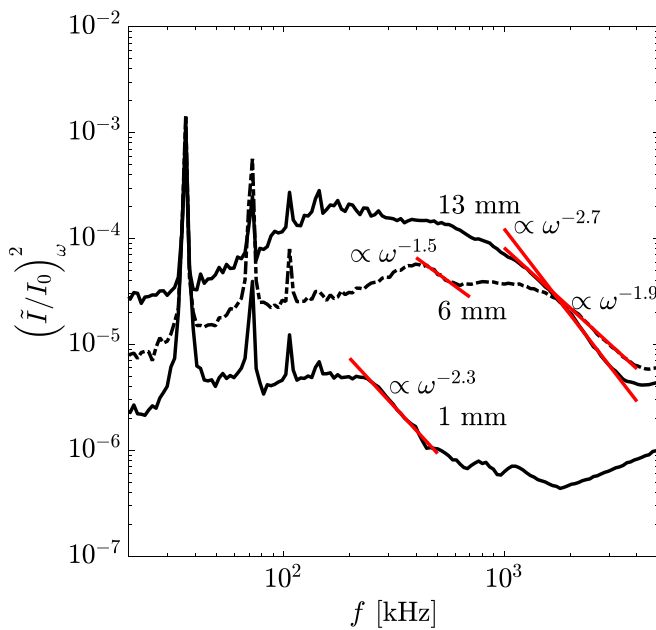


FIG. 4. Power spectra at three positions in the plume showing turbulent and coherent modes. The curve fits show scaling for high-frequency dissipation of the turbulence.

D. Dispersion relations

To show that these high-frequency waves are indeed IAT, we use a cross correlation technique^{36,37} to estimate the dispersion, $S(\omega, k)$, of the plasma and compare it to the quasilinear dispersion relation for the current-driven IAT. Here, ω is the frequency and k is the wavenumber of a propagating plane wave. This technique relies on taking a Fourier decomposition of the signals acquired from two spatially separated probes to estimate the wavenumber for each frequency in the spectrum. We then bin the domain into frequency and wavenumber bins, 5 kHz and 20 m^{-1} , respectively, and assign the average Fourier amplitude to the bin. This calculation is conducted on 2000 data sets and averaged to elevate the signal above the noise. Ultimately, the analysis results in a two-dimensional histogram, in ω and k space, where the intensity is proportional to the amplitude of each mode.

There are a number of physical and practical limitations to this approach in terms of the wavenumbers and frequency that it can measure. For example, the ion saturation current can only be used to measure plasma fluctuations below the ion plasma frequency³⁸ and therefore we have restricted our measurements to frequencies an order of magnitude below this cutoff. We also note that the wavelength resolution of this probe technique is not capable of detecting wavelengths smaller than the physical width of the probe (0.5 mm). Accordingly, we do not report measurements for wavelengths this small. Finally, our technique can only unambiguously detect wavelengths greater than the probe spacing ($\lambda_{min} = 5.2 \text{ mm} \rightarrow k_{max} = 604 \text{ m}^{-1}$). Wavenumbers that exceed k_{max} are aliased, i.e., appearing as smaller wavenumbers. This can lead to spurious results, though, we can, under certain circumstances, infer these potentially larger wavenumbers by extending the domain and using context to find patterns. We discuss the technique in greater detail in the following paragraph.

Keeping these caveats in mind, we employ this method to show in Fig. 5 a dispersion plot at a location $z = 8 \text{ mm}$ downstream of the cathode. Physically, this figure is a statistical representation of the relative amplitude of propagating plane waves in the plasma at a given frequency and wavenumber. Here, we note that we have corrected this plot for aliasing. This is done, following Ref. 28, by duplicating the dispersion plot, shifting the wavenumbers by $2 k_{max}$ and concatenating the data set along the wavenumber axis. In Fig. 5(a), the uncorrected measurement is highlighted in red. By extending the domain, patterns in the data emerge, notably at a higher frequency, and we therefore take these modes to be shorter wavelengths spuriously aliased by our measurement technique.

The results from Fig. 5 reveal the properties of the two classes of oscillations we identified from the Fourier analysis in Fig. 4. First, we see that the high frequency modes exhibit a linear dispersion relation, i.e., a linear relationship between the frequency and wavenumber. Moreover, the phase velocity of this higher frequency oscillation is given approximately by $v_{ph} = \omega/k = 4.0 \pm 0.5 \text{ km/s}$. This value is actually commensurate with the ion sound speed in this drifting plasma and indicates that, in agreement with previous work,^{28,29} this higher frequency component is a series of ion acoustic waves. Indeed, we can show that in the long wavelength limit ($k\lambda_D \ll 1$), the dispersion for ion acoustic waves is given by³⁹

$$\omega = k(u_i + c_s) \quad \text{with} \quad v_{ph} = u_i + c_s, \quad (1)$$

where $c_s = \sqrt{qT_{e0}/m_i}$ is the Bohm speed assuming cold ions and u_i is the ion drift velocity. Note, here we have used the convention that a

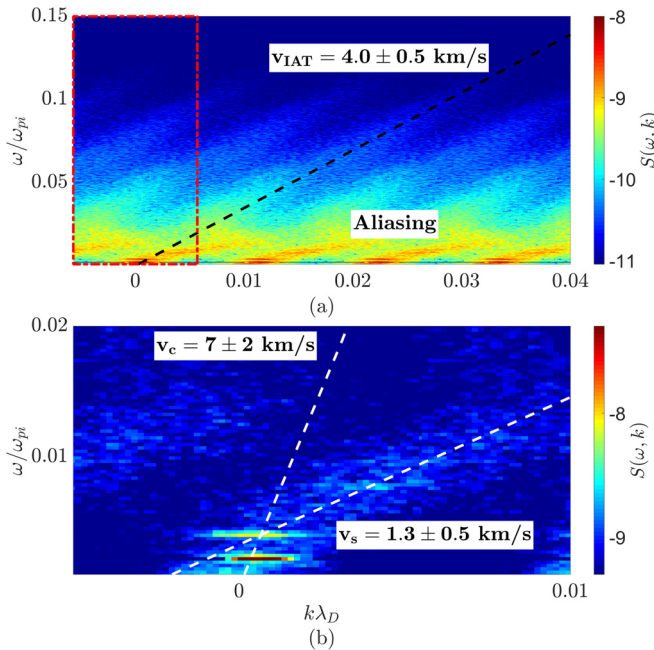


FIG. 5. (a) Dispersion relation at $z = 8$ mm from the cathode exit. The red box indicates the phase-wrapped domain. (b) Low-frequency dispersion showing the coherent structure and dispersed slow waves. The figures are saturated and corrected for phase-wrapping.

positive velocity indicates propagation toward the anode. For our measured electron temperatures we infer from the dispersion the ion drift velocity, $u_i = 2.9$ km/s, which is commensurate with typical ion drift velocities for these plasmas [2–4 km/s (Refs. 29, 34, and 40)]. As such, the measured phase velocity agrees with that of an ion acoustic wave and is consistent with other measurements in similarly configured cathodes.^{17,28,29} We further note that we have measured the dispersion along the discharge axis and found that v_{IAT} is constant throughout the plume, within uncertainty.

In a departure from previous work, however, we present in Fig. 5 the first measurements of the lower frequency plume-mode oscillations. Here, we see that there is explicit structure in the dispersion that exhibits a fundamental frequency, $f_0 = 36$ kHz, along with its first harmonic, consistent with our observations in Fig. 4. Using a trend line that connects the center of each harmonic with the origin, we find that these two modes have a group velocity of $v_c = 7 \pm 2$ km/s, which is consistent, qualitatively, with our observations of light emission from the high-speed camera. Significantly, we note that although the mode and its harmonics propagate, the coherent oscillation does not appear to be a resident mode of the cathode-to-anode cavity ($v_c/\ell \neq 36$ kHz). In addition to the dispersion of the coherent oscillations, Fig. 5(b) also shows faint evidence of slowly propagating waves with an estimated group velocity $v_s = 1.3 \pm 0.5$ km/s. This oscillation is characterized by frequencies between the coherent oscillations and the IAT. Interestingly, this type of oscillation was not immediately apparent from the power spectra plots (Fig. 4) and is only revealed by the dispersion analysis. We return to a discussion of this feature in Sec. III F.

To sum up our analysis, physically, the dispersion and Fourier measurements suggest the following features for the propagating high

and low-frequency modes. There is IAT propagating from the cathode to anode, which is known to be involved in the nonclassical heating of electrons, and it coexists with a coherent instability, which is believed to be ionization related, that propagates quickly and is correlated with the light emission from the camera. However, we have yet to identify if a clear link exists between these two phenomena.

E. Single-point correlation between IAT and self-organization

As discussed in Sec. I, the IAT is known to be a critical driver for the electron dynamics in the plume of these devices. Given that we now have established that it coexists with the coherent oscillations, we next turn to the question of a possible correlational link between the two types of waves. To this end, we choose to represent the average “energy” of the IAT with the characteristic amplitude and monitor this parameter on the time scale of the low-frequency oscillation. For the coherent oscillation, we examine the coherent component of the ion saturation current. We then compare variations in the average IAT amplitude and ion saturation current in time to determine if these parameters are correlated.

As such, we define an average amplitude of the IAT contribution to the power spectrum, \mathcal{A} , as

$$\mathcal{A} = \sum_{\omega} \left(\frac{\tilde{I}}{I_0} \right)_{\omega}^2, \quad (2)$$

where we summed over the range of the power spectrum associated with the IAT ($f > 0.02 \omega_{pi}$), excluding those lower frequency modes. We then evaluate the time evolution of the IAT amplitude by employing a series of sequential short-time Fourier transforms of the probe signal and a phase-averaging technique. We use peaks in the discharge current (detected after applying a narrow bandpass filter) as the reference in phase to perform our phase sensitive averaging. For our reported results, we used this technique to identify 5000 distinct cycles of the lower frequency, plume mode oscillation. Within each cycle, we then created a window in time over which we computed the average ion saturation current, $\langle I \rangle_{\tau}(t)$, and calculated an FFT to find the IAT amplitude, $\mathcal{A}(t)$. The window we used was $\tau = 1/(10f_0)$, where f_0 is the fundamental frequency of the plume mode oscillation. We then slid this window in time over the cycle, sampling the waveform 100 times to generate our plots. At each point in the cycle, we assigned the calculated average and FFT values to a phase defined with respect to the peak in discharge current. In this way, for each cycle, we generated 100 points as a function of phase over the period of oscillation. The reported data at each phase thus consists of the average and standard deviation of 5000 cycles.

Representative results of this analysis are shown in Fig. 6 at $z = 8$ mm. This figure depicts both the time-dependence of the turbulent ($\mathcal{A}/\mathcal{A}_0$) and coherent ($\langle \tilde{I} \rangle_{\tau}/I_0$) components of the probe signal. Since our analysis only retains one period, we have concatenated three cycles to more clearly show the waveform. Two limitations of this triggered-averaging approach stem from the variance in phase and shape of the discharge current and ion saturation measurements between cycles. To reflect how this nonconstant behavior can impact the averaged measurement, we also show the standard deviation as the gray bands in Fig. 6, which is calculated from the variance in the 5000 points within each time bin. Allowing for this uncertainty, we note that our results demonstrate that the IAT and ion saturation current

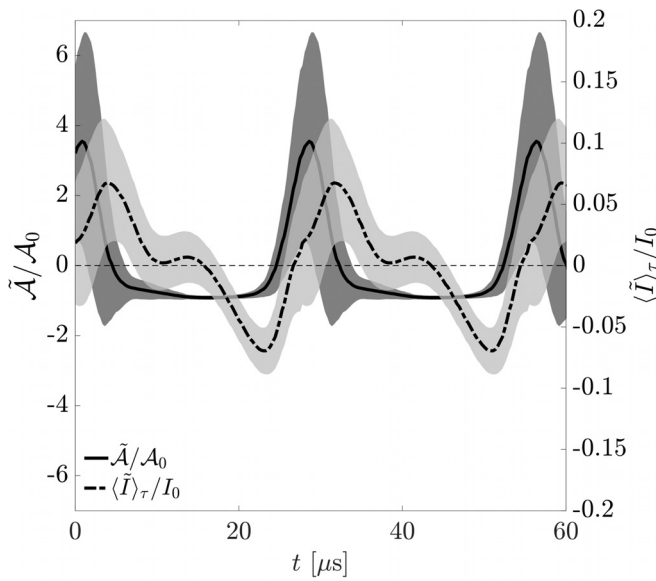


FIG. 6. Relative fluctuations in the IAT amplitude (solid) and ion saturation current (dashed) at $z = 8$ mm. The gray bands indicate the standard deviations.

fluctuations are highly correlated in time. The peak-to-peak amplitude of the IAT is an order of magnitude larger than the ion current and it unambiguously leads them in phase. This relationship is valid throughout the plume where, on average, the IAT leads the density by $\theta = 75^\circ \pm 15^\circ$ as calculated by cross correlation.

Physically, this result shows, for the first time, that the amplitude of the IAT modes is modulated in time at 36 kHz and is correlated with the characteristic coherent oscillation of the self-organized, plume-mode structure. With that said, these are single point measurements, and it remains to be seen if this correlation persists throughout the plume. To evaluate this, we turn in Sec. III F to spatially resolved measurements of these parameters and compare them with the light emission measured by the high-speed camera.

F. Spatial correlation between the IAT and self-organization

Beyond this single point measurement, we employed the same triggering technique to reconstruct the spatiotemporal evolution of the relative fluctuations of the IAT and ion saturation. We plot these results separately in Fig. 7 where we show (a) the fluctuations in the IAT and (b) the ion saturation current over two cycles. The IAT average amplitude exhibits one dominant feature that propagates from a maximum point at $z = 8$ mm downstream of the cathode exit with speed $v = 1.5 \pm 0.5$ km/s. The speed at which this change in IAT amplitude propagates is slower than the actual velocity of the underlying IAT spectrum, $v_{\text{IAT}} = 4$ km/s (see Fig. 5). This discrepancy is a reflection of the fact that the parameter we plot is the periodic variation in the energy in the IAT modes, i.e., an amplitude modulation, which does not necessarily need to propagate at the same speed as the underlying IAT. Physically, it appears that this modulation is the critical parameter correlationally linked to the lower-frequency waves in our dispersion plot [Fig. 5(b)] propagating at the same

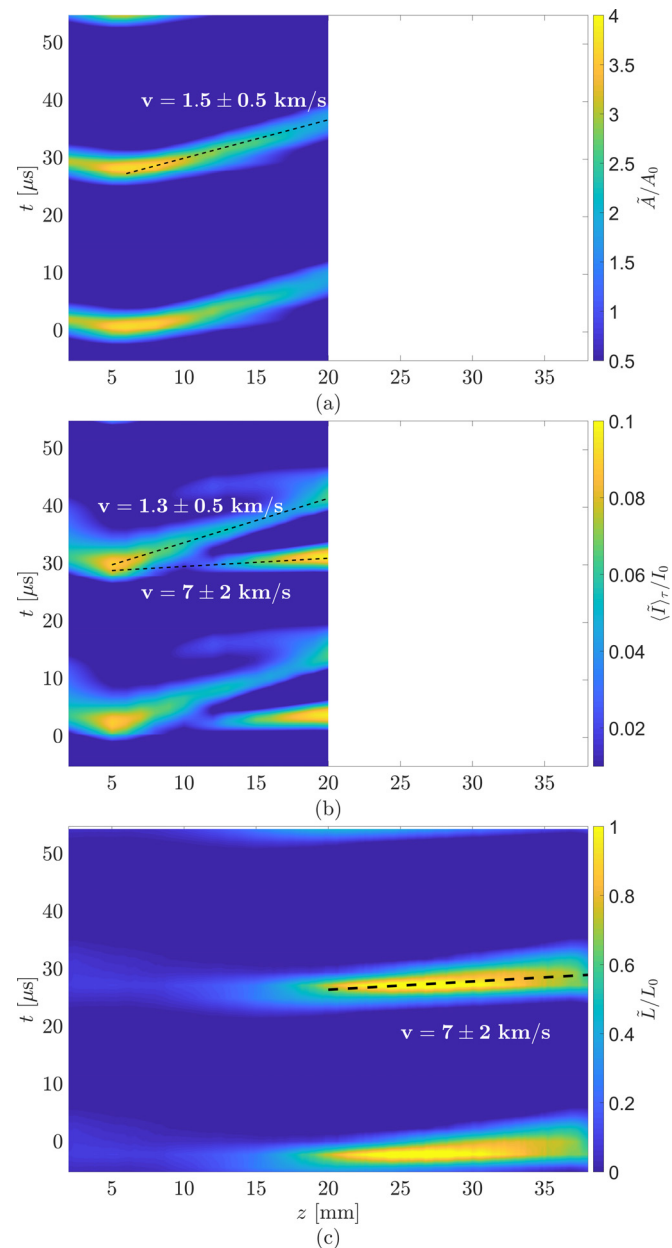


FIG. 7. (a) Evolution of IAT fluctuations along the axis of the discharge. (b) Evolution of the coherent ion saturation current fluctuations along the axis of the discharge. (c) Evolution of the radially averaged light emission. Data are interpolated and saturated to better show trends.

velocity. Furthermore, the IAT amplitude fluctuates at the same frequency as the coherent mode. To this point, these coherent oscillations $\langle \tilde{I} \rangle_\tau / I_0$ in the ion saturation current in Fig. 7(b) exhibit two features that appear to be linked in space and time with the IAT. The first is a perturbation that originates at $z = 8$ mm. As the modulation in IAT amplitude propagates through the plasma, the density lags behind. This result further supports the correlational link between the IAT and

the self-organized mode throughout the length of the cathode plume. On the other hand, the ion saturation current exhibits a second feature not observed in the IAT plot: a faster moving branch which appears further downstream and moves at a higher speed (7 km/s). This component of the plasma oscillation is correlated with the more coherent harmonic structure (peaks in Fig. 4) and the high-velocity coherent structure in the dispersion shown in Fig. 5(b). Indeed, it is this contribution that we visually associate with the coherent plume-mode oscillations from the high-speed camera.

To illustrate this, we find in Fig. 7(b) that the evolution of this faster branch in $\langle \tilde{I} \rangle_t / I_0$, is markedly similar to the light emission captured by the high-speed camera in Fig. 3. Figure 7(c) shows similar trends in the relative fluctuations in light emission, \tilde{L}/L_0 , where \tilde{L} is the fluctuation in light emission and L_0 is the time-averaged light emission. To calculate these parameters, we reconstructed a triggered-average cycle for each pixel in the image using 350 periods and averaged the result along the radial direction. To sync the camera with the probe measurements, we have set the maximum of the IAT modulation and light emission to occur at $t = 0 \mu\text{s}$. From the camera, we see that the perturbation generates light emission that is propagating at $7 \pm 2 \text{ km/s}$, in agreement with the velocity of the coherent structure in Fig. 5(b) and the high-speed component in Fig. 7(b). Notably, however, the slow branch found in the turbulence and density does not appear to generate measurable light emission. This may be due to experimental limitations in the sensitivity of the high-speed camera.

Together Figs. 7(a)–7(c) support the correlation of the large-scale self-organized mode with oscillations in the average IAT amplitude. Physically, these figures point to the plasma being perturbed by a modulation in the amplitude of the IAT modes at a fixed location, which then responds with a self-organized, low-frequency, propagating structure that results in the observed light emission. As the region of high IAT amplitude propagates in the plasma, the plasma density responds in kind.

The results in Figs. 5–7 provide a new, fundamental insight into the potential link between turbulence and self-organization. Moreover, the fact that the wave in the IAT amplitude leads the large-scale oscillations in phase suggests that the link may also be causal. Although this phase relationship is a necessary criterion to suggest that the IAT may promote the self-organized mode, it is not sufficient. To provide some context, we do note that a number of theoretical frameworks have anticipated this type of correlational and causal relationship. For example, Bychenkov *et al.*¹⁶ speculated that the growth of the IAT may give rise to time-resolved hydrodynamic effects by impacting the macroscopic transport properties of the plasma. In this case, one plausible explanation is that the IAT may enhance Ohmic heating,⁴¹ which in turn could promote additional ionization and the onset of this self-organized mode. This type of process is under active numerical investigation^{12,42} and may explain the strong correlation with the periodic light emission in Fig. 3. In Sec. IV, we expand upon this interpretation by developing a simple zero-dimensional model for the electron energy balance to interpret the amplitude and phase relationship between the IAT amplitude and the coherent oscillation.

IV. ELECTRON ENERGY MODEL

Despite the clear correlation between the IAT-driven heating and the plume mode oscillation, the causal link between the two remains unclear. To explore this potential connection, we follow the previous

theoretical and numerical work of Refs. 12, 16, and 42 and consider a here a zero-dimensional fluid model, informed by our experimental observations to interpret our results. From our measurements, we find that although the instability propagates, there is a point where the structure is almost stationary. In light of this observation, we choose to neglect spatial dependence and evaluate this zero-dimensional to this position ($z = 8 \text{ mm}$). Moreover, as this is consistent with the previous numerical and experimental work,^{12,28,29,43} we assume that turbulent resistive heating and ionization dominate the dynamics in the cathode plume. Under these simplifying assumptions, we write the electron energy equation as

$$\frac{\partial n T_e}{\partial t} = Q_{an} - n \nu_{ion} \epsilon_{ion}, \quad (3)$$

where $m_e u_e$ are the electron mass and drift velocity, Q_{an} is the Ohmic heating due to turbulence, and ν_{ion} and ϵ_{ion} are the ionization rate and energy. The anomalous resistive heating can be determined from the properties of the IAT⁴¹ as

$$Q_{an} = n m_e u_e^2 \frac{W}{n T_e} \omega_{pe} \sim n m_e u_e^2 \omega_{pe} \mathcal{A}, \quad (4)$$

where W is the wave energy density of the IAT and ω_{pe} is the electron plasma frequency. This relationship implies that greater turbulence and kinetic energy, leads to increased heating. We estimate this quantity experimentally through the average IAT amplitude, \mathcal{A} . To arrive at this relationship, we have assumed that the ion saturation current oscillations are proportional to those in density and used the Boltzmann relation connecting the density fluctuations and potential.⁴⁴ Both of these assumptions are valid when density and temperature fluctuations are small relative to their steady state values and we furthermore require the temperature fluctuations to be small compared to the density.

We supplement Eqs. (3) and (4) with the ion continuity equation,

$$\frac{\partial n}{\partial t} = n (\nu_{ion} - \nu_{ion,0}), \quad (5)$$

where $\nu_{ion,0}$ represents the steady-state ionization rate. This set of equations allows the turbulent heating of the plasma to fluctuate and to dissipate that energy through ionization, thereby increasing the density. Equation (3) is the balancing electron pressure with Ohmic heating from the turbulence and inelastic cooling from ionization. Equation (5) relates the changes in temperature to those in density through ionization. If the process we attribute to these equations holds true, then physical intuition tells us that the fluctuations in wave heating should lead the density in phase.

Having established this physical picture, we now combine Eqs. (3) and (5) under the assumption that $T_e \ll \epsilon_{ion}$ ⁴⁵ to can show that

$$\epsilon_{ion} \frac{\partial n}{\partial t} + n \frac{\partial T_e}{\partial t} + n \nu_{ion,0} \epsilon_{ion} = Q_{an}. \quad (6)$$

Taking a second derivative of Eq. (5) and substituting for the time derivative of temperature, we find that

$$\frac{\partial n}{\partial t} \left(\epsilon_{ion} - \frac{\nu_{ion}}{\gamma_{ion}} T_{e0} \right) + \frac{T_{e0}}{\gamma_{ion}} \frac{\partial^2 n}{\partial t^2} + n \nu_{ion,0} \epsilon_{ion} = Q_{an}, \quad (7)$$

where T_{e0} is the steady state electron temperature and $\gamma_{ion} = T_{e0} / \partial \nu_{ion} / \partial T_e|_{T_{e0}}$ represents the rate at which ionization changes in

response to temperature fluctuations. Due to the exponential dependence of the ionization rate on temperature, typically $\gamma_{ion} \gg \nu_{ion}$ allowing us to simplify to

$$\epsilon_{ion} \frac{\partial n}{\partial t} + \frac{T_{e0}}{\gamma_{ion}} \frac{\partial^2 n}{\partial t^2} + n\nu_{ion,0}\epsilon_{ion} = Q_{an}. \quad (8)$$

To examine the oscillation amplitude and phase, we conduct a harmonic perturbation of this equation under the convention that $n = n_0 + \tilde{n}e^{-i\omega t}$ and apply the steady state criteria, and show that

$$\frac{\tilde{Q}_{an}}{Q_{an,0}} = \left(-i \frac{\omega}{\nu_{ion,0}} - \frac{\omega^2}{\nu_{ion,0}\gamma_{ion}\epsilon_{ion}} T_{e0} + 1 \right) \frac{\tilde{n}}{n_0}. \quad (9)$$

Fluctuations in density \tilde{n}/n_0 , can be approximated from our measurements as $\langle \tilde{I} \rangle_\tau / I_0$, under the assumption that changes in T_e are relatively small compared to the density. Experimentally, we know that $\tilde{\mathcal{A}}/\mathcal{A}_0 \gg \tilde{n}/n_0$ and therefore we make the informed simplification that $\tilde{Q}_{an}/Q_{an,0} \sim \tilde{\mathcal{A}}/\mathcal{A}_0$. Therefore,

$$\frac{\tilde{\mathcal{A}}}{\mathcal{A}_0} \approx \left(-i \frac{\omega}{\nu_{ion,0}} - \frac{\omega^2}{\nu_{ion,0}\gamma_{ion}\epsilon_{ion}} T_{e0} + 1 \right) \frac{\langle \tilde{I} \rangle_\tau}{I_0}. \quad (10)$$

Examining Eq. (10), we find that the IAT wave amplitude should lead the ion saturation current fluctuation on the time scale of the self-organized mode. This is consistent with the notion that turbulence heats the electrons and changes the rate of plasma production. Furthermore, we find that the ionization frequency is an important scaling factor for the frequency which is in kind with the physical picture of an ionization instability.

V. COMPARISON OF THE MODEL AND EXPERIMENT

Having developed our electron energy model, we examine the ratio of the relative amplitudes, $a_A/a_I = (\tilde{\mathcal{A}}/\mathcal{A}_0)/(\langle \tilde{I} \rangle_\tau/I_0)$, and the phase relationship, ϕ , between $\tilde{\mathcal{A}}/\mathcal{A}_0$ and $\langle \tilde{I} \rangle_\tau/I_0$ as points of comparison between the theory and experiment. Experimentally, the ratio, a_A/a_I , was calculated at $z=8$ mm using the average of the peak-to-peak and root mean square. The uncertainty is calculated using these values as bounds. The phase at this location was determined by examining the peak, zero-crossings, and minimum, of \mathcal{A} and I in Fig. 6. The uncertainty is determined from the standard error of these values. Here, we use the convention that a positive phase means the turbulence leads the density. We evaluated our theory using the experimentally measured oscillation frequency and temperature while estimating the ionization rate from an analytical expression for the ionization rate-coefficient from Goebel and Katz.⁴⁵ The neutral density is calculated using

$$n_n = \frac{\dot{m}}{m_i v_n (r_0 + \alpha z)^2}, \quad (11)$$

where n_n is the neutral density, \dot{m} is the mass flow rate, v_n is the neutral velocity, r_0 is the orifice radius, and α is the angle of expansion. We estimate the neutral velocity as the neutral thermal speed $\sqrt{8/\pi k_B T_n/m_i}$. We have taken the neutral temperature to be between room temperature (300 K) and the insert temperature (1100 K). Here, we have shown results when $T_n = 700$ K. The half angle of expansion, α , is estimated from the experimental geometry, assuming conical

TABLE I. Comparison of measured and theoretical scaling between wave heating and density oscillations at $z=8$ mm. A positive phase implies that the heating leads to the density.

Parameter	Measured	Theory
a_A/a_I	34 ± 2	39 ± 10
ϕ	$87^\circ \pm 20^\circ$	$91^\circ \pm 1$

expansion of the plasma from the cathode to anode. The overall uncertainty in the model calculated from these bounds.

As indicated by the results in Table I, we find a quantitative agreement between our zero dimensional model and the experiment at this position in the plume. This agreement supports the following interpretation of our results. When the ionization rate is low compared to the frequency of oscillation, large changes in the IAT amplitude are necessary for relatively small changes in density. Meaning, the changes in heating are only able to effectively change the density when the steady-state ionization rate is high. In this limit, where the ionization rate is low, we find that the density and IAT should be 90° out of phase. This reflects the notion that when the IAT heats the plasma relatively quickly, the electron temperature will be in phase with the IAT amplitude. The relationship to density is then driven by how Eq. (5) relates density to ionization and temperature.

Although we are successful in qualitatively describing the global scaling between $\tilde{Q}_{an}/Q_{an,0}$ and \tilde{n}/n_0 , it does not provide information about the spatial evolution of the propagation once formed nor a dispersion relation with an onset criterion for the coherent wave. With that said, the marked agreement between our model and the experiment supports the conclusion of others^{12,42} that this self-organization is likely the result of a hydrodynamic instability driven by turbulence.

VI. CONCLUSION

In conclusion, we examined the connection between IAT and self-organized coherent oscillations in an unmagnetized current-carrying plasma. By employing ion saturation probes, we measured high-frequency turbulence and low-frequency coherent fluctuations associated with the self-organization of the plasma. Using a cross correlation technique, we estimated the dispersion and found that the high-frequency content is well described by the IAT, which coexists with a coherent mode. Applying a triggered-averaging technique, we found that the amplitude of the IAT modes is modulated in time and correlated with the coherent, large-scale ion saturation current oscillations and periodic light emission. Indeed, we have shown that turbulence can be linked correlationaly and potentially causally due to the poorly understood process of self-organization in these systems. To interpret our result, we developed a zero-dimensional model based on Ohmic heating from turbulence and dissipation through ionization. The agreement between this simple model and measured wave properties supports the notion that this self-organized mode is a hydrodynamic instability driven by turbulence.

ACKNOWLEDGMENTS

The authors acknowledge the support of the National Aeronautics and Space Administration and the Space Technology Research Fellowship Grant No. NNX15AQ37H for this work. M.

Georgin would like to thank Sarah Cusson, Ethan Dale, Zachariah Brown, and Shadrach Hepner for proofreading this manuscript.

REFERENCES

- ¹A. Hasegawa and M. Wakatani, *Phys. Rev. Lett.* **59**, 1581 (1987).
- ²K. Hallatschek and D. Biskamp, *Phys. Rev. Lett.* **86**, 1223 (2001).
- ³A. Fujisawa, K. Itoh, H. Iguchi, K. Matsuoka, S. Okamura, A. Shimizu, T. Minami, Y. Yoshimura, K. Nagaoka, C. Takahashi, M. Kojima, H. Nakano, S. Ohsima, S. Nishimura, M. Isobe, C. Suzuki, T. Akiyama, K. Ida, K. Toi, S.-I. Itoh, and P. H. Diamond, *Phys. Rev. Lett.* **93**, 165002 (2004).
- ⁴G. Dif-Pradalier, G. Hornung, P. Ghendrih, Y. Sarazin, F. Clairet, L. Vermare, P. Diamond, J. Abiteboul, T. Cartier-Michaud, C. Ehrlacher, D. Estve, X. Garbet, V. Grandgirard, D. Grcan, P. Hennequin, Y. Kosuga, G. Latu, P. Maget, P. Morel, C. Norscini, R. Sabot, and A. Storelli, *Phys. Rev. Lett.* **114**, 085004 (2015).
- ⁵A. Hasegawa and K. Mima, *Eur. Phys. J. H* **43**, 499 (2018).
- ⁶W. Wan and G. Lapenta, *Phys. Rev. Lett.* **100**, 035004 (2008).
- ⁷F. Ebrahimi and R. Raman, *Phys. Rev. Lett.* **114**, 205003 (2015).
- ⁸M. Guyot and C. Hollenstein, *Phys. Fluids* **26**, 1596 (1983).
- ⁹C. Hollenstein and M. Guyot, *Phys. Fluids* **26**, 1606 (1983).
- ¹⁰S. Tsikata and T. Minea, *Phys. Rev. Lett.* **114**, 185001 (2015).
- ¹¹I. Adamovich, S. D. Baalrud, A. Bogaerts, P. J. Bruggeman, M. Cappelli, V. Colombo, U. Czarnetzki, U. Ebert, J. G. Eden, P. Favia, D. B. Graves, S. Hamaguchi, G. Hieftje, M. Hori, I. D. Kaganovich, U. Kortshagen, M. J. Kushner, N. J. Mason, S. Mazouffre, S. M. Thagard, H.-R. Metelmann, A. Mizuno, E. Moreau, A. B. Murphy, B. A. Niemira, G. S. Oehrlein, Z. L. Petrovic, L. C. Pitchford, Y.-K. Pu, S. Rauf, O. Sakai, S. Samukawa, S. Starikovskiaia, J. Tennyson, K. Terashima, M. M. Turner, M. C. M. van de Sanden, and A. Vardelle, *J. Phys. D: Appl. Phys.* **50**, 323001 (2017).
- ¹²G. Sary, L. Garrigues, and J.-P. Boeuf, *Plasma Sources Sci. Technol.* **26**, 055008 (2017).
- ¹³G. Y. Antar, *Phys. Rev. Lett.* **91**, 055002 (2003).
- ¹⁴H. Xia and M. G. Shats, *Phys. Rev. Lett.* **91**, 155001 (2003).
- ¹⁵T. Sato and H. Okuda, *Phys. Rev. Lett.* **44**, 740 (1980).
- ¹⁶V. Y. Bychenkov, V. P. Silin, and S. A. Uryupin, *Phys. Rep.* **164**, 119 (1988).
- ¹⁷B. F. M. Pots, J. J. H. Coumans, and D. C. Schram, *Phys. Fluids* **24**, 517 (1981).
- ¹⁸K. Nishikawa and C.-S. Wu, *Phys. Rev. Lett.* **23**, 1020 (1969).
- ¹⁹K. Nishihara and A. Hasegawa, *Phys. Rev. Lett.* **28**, 424 (1972).
- ²⁰N. T. Karatzas, A. J. Anastassiadis, and K. Papadopoulos, *Phys. Rev. Lett.* **35**, 33 (1975).
- ²¹M. Yamada and M. Raether, *Phys. Fluids* **18**, 361 (1975).
- ²²T. Fukuyama, K. Taniguchi, and Y. Kawai, *Phys. Plasmas* **9**, 1570 (2002).
- ²³K. Tochigi, S. Maeda, and C. Hirose, *Phys. Rev. Lett.* **57**, 711 (1986).
- ²⁴D. Arbel, Z. Bar-Lev, J. Felsteiner, A. Rosenberg, and Y. Z. Slutsker, *Phys. Rev. Lett.* **71**, 2919 (1993).
- ²⁵D. Arbel, Z. Bar-Lev, J. Felsteiner, A. Rosenberg, and Y. Z. Slutsker, *Phys. Rev. Lett.* **78**, 66 (1997).
- ²⁶R. O. Jung, T. E. Stone, J. B. Boffard, L. W. Anderson, and C. C. Lin, *Phys. Rev. Lett.* **94**, 163202 (2005).
- ²⁷D. M. Goebel, K. K. Jameson, I. Katz, and I. G. Mikellides, *Phys. Plasmas* **14**, 103508 (2007).
- ²⁸B. A. Jorns, I. G. Mikellides, and D. M. Goebel, *Phys. Rev. E* **90**, 063106 (2014).
- ²⁹B. A. Jorns, C. Dodson, D. M. Goebel, and R. Wirz, *Phys. Rev. E* **96**, 023208 (2017).
- ³⁰T. R. Sarver-Verhey, H. Kamhawi, D. M. Goebel, J. E. Polk, P. Y. Peterson, and D. A. Robinson, in *52nd AIAA/SAE/ASEE Joint Propulsion Conference* (American Institute of Aeronautics and Astronautics, Salt Lake City, UT, 2016).
- ³¹E. Chesta, C. M. Lam, N. B. Meezan, D. P. Schmidt, and M. A. Cappelli, *IEEE Trans. Plasma Sci.* **29**, 582 (2001).
- ³²T. A. Carter, B. Brugman, P. Pribyl, and W. Lybarger, *Phys. Rev. Lett.* **96**, 155001 (2006).
- ³³S. Dorfman and T. A. Carter, *Phys. Rev. Lett.* **110**, 195001 (2013).
- ³⁴G. Williams, T. B. Smith, M. T. Domonkos, A. D. Gallimore, and R. P. Drake, *IEEE Trans. Plasma Sci.* **28**, 1664 (2000).
- ³⁵T. Honzawa and Y. Kawai, *Plasma Phys.* **14**, 27 (1972).
- ³⁶D. B. Ilić, *Phys. Fluids* **20**, 1717 (1977).
- ³⁷J. M. Beall, Y. C. Kim, and E. J. Powers, *J. Appl. Phys.* **53**, 3933 (1982).
- ³⁸B. Nold, T. T. Ribeiro, M. Ramisch, Z. Huang, H. W. Müller, B. D. Scott, U. Stroth, and ASDEX Team, *New J. Phys.* **14**, 063022 (2012).
- ³⁹T. H. Stix, *The Theory of Plasma Waves* (AIP, 1962).
- ⁴⁰C. A. Dodson, D. Perez-Grande, B. A. Jorns, D. M. Goebel, and R. E. Wirz, *J. Propul. Power* **34**, 1225 (2018).
- ⁴¹R. Z. Sagdeev and A. A. Galeev, *Nonlinear Plasma Theory* (W. A. Benjamin, 1969).
- ⁴²I. G. Mikellides, P. Guerrero, A. Lopez Ortega, and J. E. Polk, in *54th AIAA/ASME/SAGE/ASEE Joint Propulsion Conference* (2018), p. 4722.
- ⁴³A. L. Ortega, B. A. Jorns, and I. G. Mikellides, *J. Propul. Power* **34**, 1026 (2018).
- ⁴⁴B. A. Jorns, I. G. Mikellides, and D. M. Goebel, in *50th AIAA/ASME/SAGE/ASEE Joint Propulsion Conference* (2014), p. 3826.
- ⁴⁵D. M. Goebel and I. Katz, *Fundamentals of Electric Propulsion: Ion and Hall Thrusters* (John Wiley & Sons, 2008), Vol. 1.